

Phase diagram for freeze-dried persimmon

P.J.A. Sobral^{a,*}, V.R.N. Telis^b, A.M.Q.B. Habitante^a, A. Sereno^c

^aUniversidade de São Paulo, FZEA-ZAZ-CP 23, 13630-000 Pirassununga, SP, Brazil

^bDepartment of Food Engineering and Technology, Universidade Estadual Paulista, Alimentos 15054-090, São José do Rio Preto, SP, Brazil

^cFaculdade de Engenharia, Department of Chemical Engineering Química, Universidade do Porto, 4200-465 Porto, Portugal

Received 27 December 2000; received in revised form 17 April 2001; accepted 19 April 2001

Abstract

Phase transitions of freeze-dried persimmon in a large range of moisture content were determined by differential scanning calorimetry (DSC). In order to study this transitions at low and intermediate moisture content domains, samples were conditioned by adsorption at various water activities ($a_w = 0.11$ – 0.90) at 25°C . For the high moisture content region, samples were obtained by water addition. At $a_w \leq 0.75$ two glass transitions were visible, with T_g decreasing with increasing water activity due to water plasticizing effect. The first T_g is due to the matrix formed by sugars and water. The second one, less visible and less plasticized by water, is probably due to macromolecules of the fruit pulp. At a_w between 0.80 and 0.90 a devitrification peak appeared after T_g and before T_m . At this moisture content range, the Gordon–Taylor model represented satisfactorily the matrix glass transition curve. At the higher moisture content range ($a_w > 0.90$), the more visible phenomenon was the ice melting. T_g appeared less visible because the enthalpy change involved in glass transition is practically negligible in comparison with the latent heat of melting. In the high moisture content domain T_g remained practically constant around $T_g' (-56.6^\circ\text{C})$. © 2001 Elsevier Science B.V. All rights reserved.

Keywords: Persimmon; Glass transition; Differential scanning calorimetry; Water activity; Sorption isotherm

1. Introduction

The physical state of foods, including sugars and biopolymers, has received increasing attention because of its importance to food processing and storage [1,2]. In the Food Polymer Science, one of the most important properties used to characterize the physical state is the glass transition, which involves transition from a “glassy” solid to a “rubbery” liquid-like state [1,3,4]. This change occurs within a temperature range characteristic for each material and the mid-point temperature of such change is taken as the

glass transition temperature (T_g). Because there is an important increase on molecular mobility across T_g , this glass transition temperature is hypothesized to be an important parameter for storage stability and quality of dried or frozen products [5,6].

According to Karmas et al. [7], non-enzymatic browning phenomena are affected by glass transition. Fan et al. [8] discussed the role of the glass transition in determining product density and shape of extrudates. Some authors have studied the effect of drying and/or osmotic dehydration on glass transition of apples [9,10], tomatoes [11] and other plant materials [12]. Others have studied frozen products [5,13].

In the case of frozen food, there is another important property, called the glass transition of the maximally freeze-concentrated glass (T_g'). The minimal moisture

* Corresponding author. Fax: +55-19-5611-689.
E-mail address: pjsobral@usp.br (P.J.A. Sobral).

Nomenclature

a_w	water activity
C	parameter in Eq. (1)
ΔH_{de}	enthalpy of devitrification (J g^{-1})
ΔH_m	enthalpy of ice melting (J g^{-1})
k, k'	parameters in Eqs. (2) and (5), respectively
K	parameter in Eq. (1)
q	parameter in Eq. (5)
r^2	correlation coefficient
T_d	peak devitrification temperature ($^{\circ}\text{C}$)
T_g	midpoint glass transition temperature (K)
T'_g	glass transition temperature of the maximally freeze-concentrated material ($^{\circ}\text{C}$)
T_{gs}	glass transition temperature of the dry solids (K)
T_{gw}	glass transition temperature of pure water (K)
T_m	onset melting temperature ($^{\circ}\text{C}$)
X'_g	water fraction of the maximally freeze-concentrated material (gram water per gram moist solids)

content where T'_g is visible corresponds to the unfreezable water content (X'_g). According to Franks [14], depending on the rate of cooling, the system will consist of ice crystals embedded in an amorphous glass matrix that has a characteristic glass/rubber transition temperature, T'_g , above which it begins to lose quality. The breakdown of structure above a “collapse” temperature (which is related to T_g) during freeze-drying is considered to be a major contributor to deteriorating product quality [12,15].

Water has a strong plasticizing effect on the food matrix [1]. Thus, normally, the glass transition temperature is plotted versus moisture content of product, forming the glass transition curve. When the melting temperature versus moisture content is also added to the same plot, a state diagram is obtained [16–18]. Glass transition curves of animal [5,19,20] or vegetal [6,8,11,12] products are relatively abundant in literature. State diagrams for aqueous solutions of pure components and model systems are also easily found in literature: sugars [1,16], starch hydrolysis products

[21], and proteins [22]. However, quantitative data for natural foods are relatively scarce. Complete state diagrams for this kind of material are found only for onion, grape and strawberry [23,24], apple [9,10] and pineapple [25,26].

Persimmon is a fruit produced in Brazil since the last century that begins to interest industry [27,28]. Relevant property data for dehydration industry [27] and for storage under refrigeration [28] may be found in literature, but not for the freezing industry. So, the objective of this work was to study the phase transitions of freeze-dried persimmon and to draw the corresponding state diagram for this material.

2. Materials and methods

Persimmon (*Diospyros kaki* L.) used in this study was obtained at the local market. The fruits were hand peeled, cored and picked, being immediately frozen by immersion in liquid nitrogen and freeze-dried in a Heto HD1 (Heto Lab Equipment).

To obtain results in the hygroscopic domain, freeze-dried samples (1.0–1.6 g) were equilibrated over saturated salt solutions (LiCl , MgCl_2 , K_2CO_3 , $\text{Mg}(\text{NO}_3)_2$, NaNO_2 , NaCl , $(\text{NH}_4)_2\text{SO}_4$, KCl , BaCl_2) to maintain the water activity (a_w) between 0.11 and 0.90, at 25°C ($\pm 0.2^{\circ}\text{C}$) for 2–3 weeks [29]. To analyze samples with higher water activities ($a_w > 0.90$), the freeze-dried samples were mixed with distilled water in order to obtain 55–90% moisture content (w.b.). These samples were equilibrated at 4°C for 24 h before differential scanning calorimetry (DSC) analysis [26]. Their water activity was determined at 25°C , with the help of an AquaLab CX2 (Decagon Devices Inc.).

For DSC analysis, equilibrated samples of about 10 mg conditioned in hermetic TA aluminum pans, were heated at $10^{\circ}\text{C min}^{-1}$, between -120 and 100°C , in inert atmosphere (100 ml min^{-1} of N_2) in a DSC TA2010 controlled by a TA5000 module (TA Instruments, New Castle, DE, USA). The reference was an empty aluminum pan. Liquid nitrogen was used for sample cooling before the run. Freeze-dried samples without preconditioning were also analyzed. The remaining material was used for determining the moisture content of samples, accomplished by drying in a vacuum laboratory oven at 100 mmHg and 95°C , for 48 h.

When a devitrification peak occurred, the samples were annealed at the devitrification peak temperature for 30 or 60 min before the second scan. The midpoint temperature of glass transition (T_g), peak temperature of devitrification (T_d), onset temperature of ice melting (T_m), and devitrification (ΔH_{de}) and ice melting (ΔH_m) enthalpies were determined from the DSC curves with the help of the software Universal Analysis V1.7F (TA Instruments). All analyses were obtained in triplicate. All weighing (± 0.1 mg) was accomplished on analytical balance (SA210, Scientech).

All regressions were made with the help of Statistica software V.1.1.5 using the Quasi-Newton method [30].

3. Results and discussion

Sample conditioning allowed to relate the equilibrium moisture content with the respective water activity at 25°C. These experimental points, obtained in triplicate, are presented in Fig. 1. The shape of the isotherm in the whole domain of water activity was similar to that of pineapple previously obtained in a similar work [26]. The behavior of data obtained by adsorption ($a_w \leq 0.90$) was identical to those observed by Telis et al. [27] that determined absorption isotherms

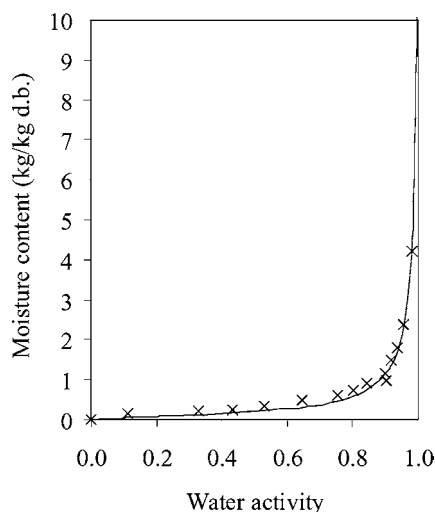


Fig. 1. Sorption isotherm of freeze-dried persimmon at 25°C; Eq. (1).

of skin and pulp of persimmon between 20 and 70°C. However, in the present work the product seemed to be more hygroscopic. The monolayer moisture content, calculated by fitting ($r^2 = 0.995$) the Guggenheim–Anderson–De Boer (GAB) model (Eq. (1)) was 13.1% (d.b.) while Telis et al. [27] obtained 10.9% and 11.3% (d.b.) for persimmon pulp and skin, respectively.

$$\frac{X_{ws}}{X_m} = \frac{CKa_w}{(1 - Ka_w)(1 - Ka_w + CKa_w)} \quad (1)$$

In Eq. (1), X_{ws} is the moisture content in dry basis and a_w the water activity. The GAB parameters C and K , which are associated with the monolayer and multilayer enthalpies, were calculated as 3.415 and 0.989, respectively.

The results of DSC analyses presented different behaviors for each water activity domain. At $a_w \leq 0.75$ two glass transitions were visible (Fig. 2) as a deviation in base line and shifted toward lower temperatures with increasing moisture content and water activity, due to plasticizing effect of water [3]. The first one, well visible at lower temperatures, corresponds to the glass transition of a matrix formed by sugars and water. The second one, less visible and less plasticized by water, is probably due to macromolecules of the fruit pulp. Two glass transitions are normally visible in systems formed by blends of polymers [31] and in edible films based on proteins [32,33], due to phase separation between polymers and between proteins and plasticizers, respectively.

At a_w between 0.80 and 0.90 (Fig. 3), a well visible devitrification peak appeared after T_g and before T_m .

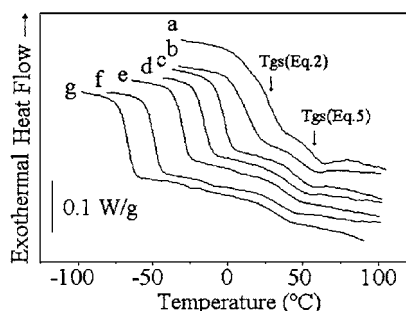


Fig. 2. DSC curves of freeze-dried persimmon in the low a_w domain: (a) 0.11; (b) freeze-dried samples without conditioning; (c) 0.33; (d) 0.43; (e) 0.53; (f) 0.64; (g) 0.75.

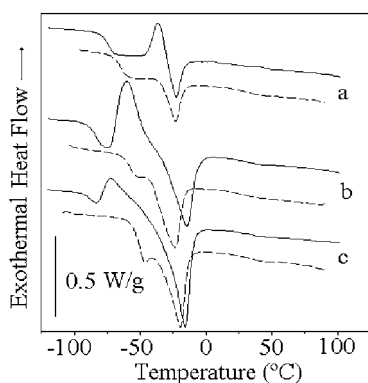


Fig. 3. DSC curves of freeze-dried persimmon in the intermediate a_w domain: (a) 0.80; (b) 0.83; (c) 0.90; with (---) and without (—) annealing at T_d for 30 (a, b) or 60 min (c).

This phenomenon occurred because rapid cooling resulted only in partial freeze-concentration of the solution; during rewarming the increase of water mobility caused crystallization of trapped amorphous water [1,16,21]. Similar results in the same range of water activity were obtained only by Sá et al. [10] with apples. Sá and Sereno [23] with grape, Goff [17] with diluted sucrose solutions, Roos [24] with strawberry and Telis and Sobral [25,26] with pineapple, also observed devitrification exotherms, but for samples equilibrated at $a_w \geq 0.84$.

As expected, T_d decreased as a_w increased, probably due to the plasticizing effect of moisture. However, devitrification enthalpy presented a maximum at $a_w = 0.84$ (Table 1). In a more detailed study, Telis and Sobral [26] have observed this same behavior.

These samples were submitted to isothermal annealing at T_d . Thirty minutes were sufficient to eliminate

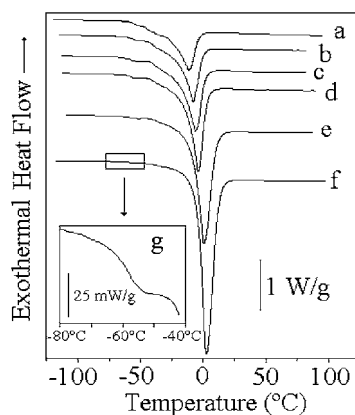


Fig. 4. DSC traces of freeze-dried persimmon in the high (>0.90) a_w domain: (a) $X_w = 54.0\%$; (b) $X_w = 59.7\%$; (c) $X_w = 64.3\%$; (d) $X_w = 70.3\%$; (e) $X_w = 80.8\%$; (f) $X_w = 90.4\%$; (g) the insert displays the glass transition of sample with $X_w = 90.4\%$ more visible (zoom).

the devitrification peak in samples conditioned at 0.80 and 0.84 of a_w , but for $a_w = 0.90$, 60 min were necessary to complete elimination of peaks (Fig. 3). As expected, T_g of annealed samples were higher than that of the non-annealed ones (Table 1), due to the greater fraction of ice formed and consequent concentration of the amorphous glassy matrix [23,25].

In the higher moisture content range ($a_w > 0.90$), the ice melting was the more visible phenomenon (Fig. 4). T_g appeared less visible, because the heat effect involved in glass transition is practically negligible in comparison with the latent heat of melting (see detail in Fig. 4). These results are similar to those obtained by Roos and Karel [13] with diluted sucrose solutions, Sá and Sereno [23] with fresh grape samples, and Telis and Sobral [26] with pineapple. In this

Table 1
Phase properties of samples conditioned between 0.80 and 0.90 of water activity^a

Properties	Water activities		
	0.80	0.84	0.90
Non-annealed samples			
Devitrification temperature (°C)	-36.7 ± 0.5	-62.8 ± 2.6	-70.2 ± 2.0
Devitrification enthalpy (J g^{-1})	12.1 ± 1.2	42.7 ± 1.4	11.7 ± 2.8
Glass transition temperature (°C)	-74.1 ± 0.8	-84.5 ± 0.6	-86.9 ± 1.0
Annealed samples			
Glass transition temperature (°C)	-64.9 ± 0.1	-56.8 ± 0.3	-49.6 ± 0.2

^a Average \pm S.D.

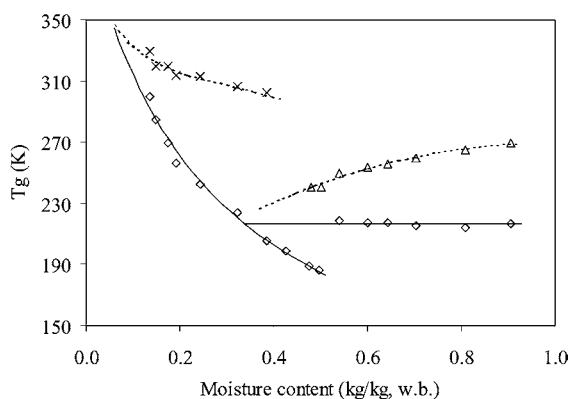


Fig. 5. State diagram of freeze-dried persimmon: (\diamond) T_g of matrix; (\triangle) T_m ; and (\times) T_g of macromolecules fraction.

last work, this behavior firstly appeared in the samples conditioned at $a_w = 0.90$.

The values of the glass transition temperature of non-annealed samples and the onset temperature of ice melting, all of them considered as the average of triplicates, plotted in function of moisture content constitute the state diagram of persimmon (Fig. 5). In the hygroscopic domain ($a_w \leq 0.9$), the plasticizing effect of water is evident, with a great reduction of the sugar matrix T_g caused by increasing moisture content and molecular mobility. At water activities higher than 0.90, the glass transition curve exhibited a discontinuity, with a sudden increase of the glass transition temperatures that approached a constant value, corresponding to the glass transition of the maximally freeze-concentrated amorphous matrix ($T_g' = 216.5 \pm 1.5$ K). Roos and Karel [13] and Telis and Sobral [26] showed similar glass transition curves obtained with diluted sucrose solution and freeze-dried pineapple, respectively. Such result led Telis and Sobral [25] to conclude that the observed T_g in freeze-dried pineapple was mainly due to its sugar content.

The glass transition curve of the sugar matrix in the hygroscopic domain is a theoretical glass curve [3] and may be represented by the Gordon–Taylor model (Eq. (2)) for binary systems (Fig. 5). The following parameters were calculated by non-linear regression: $k = 4.77$ and $T_{gs} = 406.6$ K, with $r^2 = 0.990$, using $T_{gw} = 138$ K [3]. The Gordon–Taylor constant value is the same calculated from the glass transition curve of pineapple [26] and sucrose [18]. This reinforces the

conclusion of Telis and Sobral [25] that the T_g is mainly affected by the sucrose present in the fruits.

$$T_g = \frac{X_s T_{gs} + k X_w T_{gw}}{X_s + k X_w} \quad (2)$$

As expected, the melting temperature decreased with decreasing water content. The intersection of the extrapolated ice melting and glass transition curves would be expected to occur at T_g' [1,3,23]. Considering that the empirical Eq. (3) fitted well ($r^2 = 0.982$) the experimental points of T_m , the calculated T_g' value is 218.1 K (-55.0°C) that is close to the value calculated by averaging the values of T_g (-56.6°C) in the high a_w domain.

$$T_m = 158.6 + 226.2 X_w - 115.6 X_w^2 \quad (3)$$

The ice melting enthalpy varied linearly ($r^2 = 0.984$) with moisture content of products according to Eq. (4) (Fig. 6). The extrapolation of Eq. (4) to $\Delta H_m = 0$ allowed calculation of the unfreezable water content (X_w') corresponding to the maximally freeze-concentrated material [13].

$$\Delta H_m = 460.3 X_w - 180.2 \quad (4)$$

The unfreezable water content determined through Eq. (4) was 0.39 g water per gram moist solids. The value of X_w' predicted from intersection of Eq. (2) with Eq. (3) was 0.33 and with horizontal line of $T_g' = -56.5^\circ\text{C}$ was 0.34 g water per gram moist solids. Telis and Sobral [26] also observed that the use of Eq. (4) overestimated X_w' . On the other hand, Sá

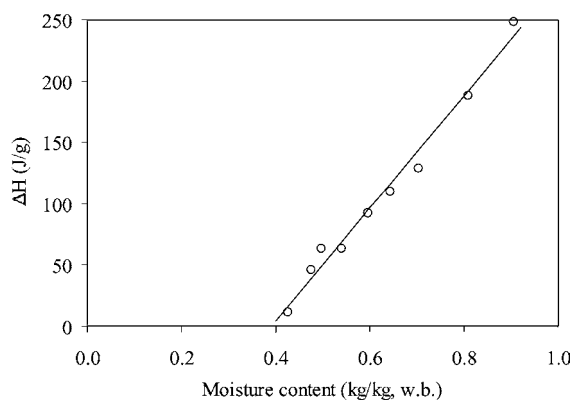


Fig. 6. Enthalpy of ice melting (ΔH_m) as function of moisture content.

and Sereno [23] observed that X'_g calculated through regression of ΔH_m versus moisture content were, in general, lower than those corresponding to T'_g values obtained from the DSC curves of annealed samples.

The glass transition observed at low and higher temperatures is supposed to be due to fruit sugars and macromolecules, respectively. In fact, the freeze-dried samples had 96.1 g of total sugars (8.0 g sucrose, 45.0 g glucose and 43.1 g fructose)/100 g of dry solids and 3.7 g of pectin/100 g of dry solids, determined in triplicate by classical methods [34,35].

The higher T_g was also reduced by water (Fig. 5), but generated a practical glass transition curve [3], in the sense that it tends to an asymptotic value other than T_{gw} . In this situation, the Kwei model (Eq. (5)) is the most appropriated to represent the experimental data.

$$T_g = \frac{X_s T_{gs} + k' X_w T_{gw}}{X_s + k X_w} + q X_s X_w \quad (5)$$

Eq. (5) could be adequately fitted to experimental points, with the following parameters calculated by non-linear regression: $k' = 4.46$, $T_{gs} = 370.3$ K and $q = 432.0$ K, with $r^2 = 0.906$. This model has been successfully used to represent practical glass transition curve of several products including fruits [25] and biopolymers [20].

4. Conclusions

Differential scanning calorimetry proved to be an adequate method to determine glass transition temperatures in freeze-dried samples of persimmon, allowing to obtain a state diagram for such material. Gordon–Taylor model could adequately represent the sugar matrix glass transition curve, while the Kwei model produced a good fit of the higher temperature transitions, which were observed with low moisture samples and were attributed to the presence of natural macromolecules behaving like a separated phase. In an intermediate moisture range ($0.80 \leq a_w \leq 0.90$) devitrification peaks were observed, which disappeared after annealing for a period ranging from 30 to 60 min. In the high moisture range, samples exhibited a constant glass transition value of -56.6°C , which corresponds to the maximally concentrated solid matrix glass transition T'_g .

Acknowledgements

To CYTED (Ibero-American Program on Science and Technology for Development), project XI.12.

References

- [1] Y. Roos, M. Karel, *J. Food Sci.* 56 (1) (1991) 38.
- [2] G.W. White, S.H. Cakebread, *J. Food Technol.* 1 (1966) 73.
- [3] L. Slade, H. Levine, *Crit. Rev. Food Sci. Nutr.* 30 (2/3) (1991) 115.
- [4] H. Levine, L. Slade, *Comments Agric. Food Chem.* 1 (6) (1989) 315.
- [5] C. Inoue, M. Ishikawa, *J. Food Sci.* 62 (3) (1997) 496.
- [6] K.J. Zeleznak, R.C. Hosney, *Cereal Chem.* 64 (2) (1987) 121.
- [7] R. Karmas, M.P. Buera, M. Karel, *J. Agric. Food Chem.* 40 (5) (1992) 873.
- [8] J. Fan, J.R. Mitchell, J.M.V. Blanshard, *Int. J. Food Sci. Technol.* 31 (1) (1996) 55.
- [9] A.M. Sereno, M.M. Sá, A.M. Figueiredo, in: C.B. Akritidis, D. Marinos-Kouris, G.D. Saravacos (Eds.), *Drying'98*, Ziti Editions, Thessaloniki, 1998, p. 1214.
- [10] M.M. Sá, A.M. Figueiredo, A.M. Sereno, *Thermochim. Acta* 329 (1999) 31.
- [11] A.F. Baroni, M.D. Hubinger, in: *Proceedings of the 12th International Drying Symposium (IDS2000)*, 2000, Paper No. 114 (CD ROM).
- [12] S.A. Anglea, V. Karathanos, M. Karel, *Biotechnol. Prog.* 9 (1993) 204.
- [13] Y. Roos, M. Karel, *J. Food Sci.* 56 (1) (1991) 266.
- [14] F. Franks, in: L. Slade, H. Levine (Eds.), *Water Relationships in Food*, Plenum Press, New York, 1991, p. 1.
- [15] G. Levi, M. Karel, *Food Res. Int.* 28 (2) (1995) 145.
- [16] Y. Roos, *J. Food Eng.* 24 (3) (1995) 339.
- [17] H.D. Goff, *Food Res. Int.* 27 (1994) 187.
- [18] Y. Roos, M. Karel, *Food Technol.* 12 (1991) 66.
- [19] J.M. Aguilera, G. Levi, M. Karel, *Biotechnol. Prog.* 9 (1994) 651.
- [20] P.J.A. Sobral, F.C. Menegalli, S. Guilbert, in: P. Colonna, S. Guilbert (Eds.), *Biopolymer Science: Food and Non Food Applications*, Les Colloques No. 91, INRA, Paris, 1998, p. 111.
- [21] H. Levine, L. Slade, *Carboh. Polym.* 6 (1986) 213.
- [22] A.M. Cocero, J.L. Kokini, *J. Rheol.* 35 (2) (1991) 257.
- [23] M.M. Sá, A.M. Sereno, *Thermochim. Acta* 246 (1994) 285.
- [24] Y. Roos, *J. Food Sci.* 52 (1) (1987) 146.
- [25] V.R.N. Telis, P.J.A. Sobral, *Braz. J. Food Technol.* 2 (1999) 181.
- [26] V.R.N. Telis, P.J.A. Sobral, *Lebensmittel-Wissens, Technol.* 34 (2001) 199.
- [27] V.R.N. Telis, A.L. Gabas, F.C. Menegalli, J. Telis-Romero, *Thermochim. Acta* 343 (1/2) (2000) 49.
- [28] M.A. de Moura, L.C. Lopes, A.A. Cardoso, L.C.G. de Miranda, *Pesq. Agropec. Brasil.* 32 (1997) 1105.

- [29] W.E.L. Spiess, W.R. Wolf, in: F. Escher, B. Hallstrom, H.S. Meffert, W.E.L. Spiess, G. Voss (Eds.), *Physical Properties of Foods*, Applied Science Publishers, New York, 1983, p. 65.
- [30] StatSoft Inc., *STATISTICA for Windows* (Computer program manual), Tulsa, StatSoft Inc., <http://www.statsoft.com>, 1995.
- [31] H. Verghoogt, B.A. Ramsay, B.D. Favis, *Polym. Rev.* 35 (1994) 5155.
- [32] S.M.A. Souza, P.J.A. Sobral, F.C. Menegalli, in: P. Colonna, S. Guilbert (Eds.), *Biopolymer Science: Food and Non Food Applications*, Les Colloques No. 91, INRA, Paris, 1998, p. 183.
- [33] N. Gontard, S. Ring, *J. Agric. Food Chem.* 44 (1996) 3474.
- [34] Office International de la Vigne et du Vin, *Recueil des méthodes internationales d'analyse des boissons spiritueuses, des alcools et de la fraction aromatique des boissons*, OIV, Paris, 1994, p. 103.
- [35] S. Ranganna, *Manual of Analysis of Fruit and Vegetable Products*, McGraw-Hill, New Delhi, 1978.